Use of Centrifuge Tests for the Validation of Innovative Concepts in Foundation Engineering

J. Garnier
Head of Soil Investigations and Soil Mechanics Division, Laboratoire Central des Ponts et Chaussées, Nantes, France

A. Pecker
Chairman Managing Director, Géodynamique et Structure, Bagneux, France

ABSTRACT: The design of important civil engineering structures often introduces new concepts which have not be validated by previous experience. Extensive use of numerical modeling may help understand the behavior of structures under extreme loading conditions. However, this modeling requires an experimental validation that only centrifuge tests may offer. This use of centrifuge tests as a validation tool is illustrated for the foundations of the Rion Antirion bridge (Greece).

1 INTRODUCTION

The design and the conception of important civil engineering structures require the use of exceptional tools for numerical modeling and experimental validation. Among the most appropriate experimental tools, model tests take up a privileged place. The complex behavior of geomaterials encountered either in foundation or in the structure itself (earth dams for instance), requires that model tests be realized with the original material. This requirement, and the strong stress dependence of the behavior of geomaterials impose that the gravity field be adequately reproduced.

This paper illustrates the contribution of centrifuge tests in the validation of a new foundation concept in seismic areas. This innovative foundation concept is presently being implemented for the Rion Antirion bridge in Greece. Coupled to extensive numerical modeling, these tests proved the validity of the concept and of the theoretical tools developed for design.

2 DESCRIPTION OF THE STRUCTURE

The Rion Antirion bridge is a unique structure which, within the framework of a B.O.T. contract, has been granted to the French Company Dumez-GTM by the Greek government. This bridge is located near Patras, 250 km west of Athens, and will constitute a fixed link between the Peloponese and the Continent. The main bridge is a three spans cabled-stayed structure, with a total length of 2 290 m; the central spans are 560 m long each. It is located in exceptional environmental conditions characterized by a deep water depth (65 m), weak foundation soils composed of alluvial deposits (alternate layers of silty sands, sandy clays and medium plasticity clays) and a high seismic design motion (peak ground acceleration of 0.48 g at the seabed level). (Combault - Morand 1998; Pecker - Teyssandier 1998)).

To accommodate these environmental conditions, the solution chosen by Dumez-GTM, the designer, consists in gravity base caissons directly founded at the seabed level (figure 1).

The foundation diameter, at the seabed level, is equal to 90 m extended by a cone with a diameter of 26 m at the sea level. The total height of one pylon is approximately 220 m among which 65 m are below water. The dead weight of one pier is of the order of 800 MN. To this permanent load, a horizontal shear force of 600 MN and an overturning moment of 20 000 MN.m.m are superimposed during the earthquake.

Figure 1: Pier Elevation

In view of the poor quality of the foundation soils, a direction foundation on the in-situ soils cannot be foreseen and some kind of soil improvement is required. The final scheme which has been chosen is presented in figure 2; it consists of stiff inclusions driven at close spacing below and outside the foundation. At the present design stage, 270 hollow steel pipes, 2 m in diameter, 20 mm thick and 25 m to 30 m long, are driven at a square mesh of 7 m x 7 m (figure 2).

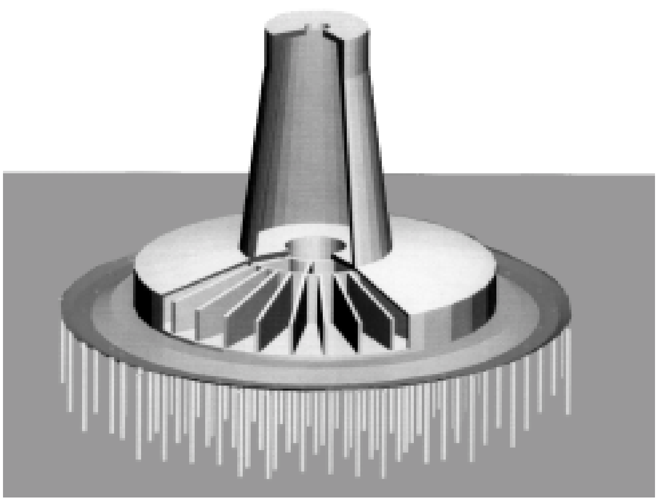

Figure 2. Pier foundation

These inclusions are not connected to the raft and a free draining gravel bed layer is laid on top of the inclusions below the raft. This layer prevents suction, allows uplift and sliding during the seismic excitation. This arrangement, which enforces a capacity design philosophy in foundation engineering (Pecker 1998) limits the forces and moments transmitted to the superstructure and to the foundation soils.

3 OBJECTIVES OF THE CENTRIFUGE TESTS

This totally innovative concept, at least in seismic areas, clearly calls for extensive theoretical analyses and experimental validation. As sophisticated as can be, the theoretical and numerical tools do not have the capacity of modeling all the details of the behavior of this complex scheme during an earthquake. Centrifuge model tests were therefore undertaken with a three-fold objective:

- validate the theoretical predictions of the ultimate bearing capacity of the foundation under monotonically increasing shear force and overturning moment,
- identify the failure mechanism of the foundation under these combined loads,
- assess the behavior of the foundation under various cyclic load paths.

4 DESCRIPTION OF THE CENTRIFUGE FACILITY AND TEST SET UP

The three tests have been performed in the 200 g-ton geotechnical centrifuge at the LCPC Nantes center. The centrifuge was described by Corte and Garnier (1986). It is designed to carry a 2000 kg payload to 100 g accelerations, the bucket surface is at a radius of 5.5 m and the platform has a working space of 1.4 m by 1.1 m.

All tests have been carried out at 100 g on models at a scale of 1/100 (Figure 3). The dimensions of the corresponding prototype are as follows :

Radius of the circular footing : $B_f = 30$ m

Inclusions: Length and diameter: D = 8.5 m and $B_i = 0.67$ m

Wall thickness t = 6.7 mm (steel)

Stiffness EI = 158 MN.m^2

Thickness of the ballast layer : 1.2 m

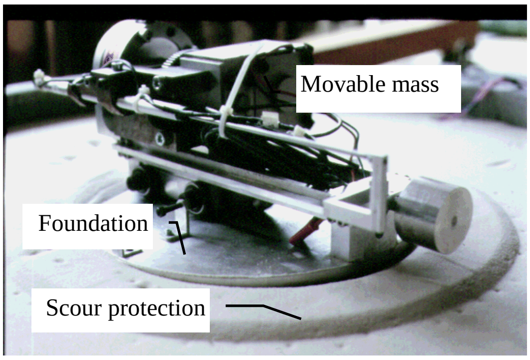

Figure 3. Model foundation (scale 1/100)

The soil material has been sampled at location of pier N17 of the Antirion approach viaduct and sent to the laboratory. The clay is dried at 60° for 24 hours, water is added to bring the water content to about w = 80% and the slurry is mixed under vacuum during 4 hours to get a homogeneous material. The slurry poured into the cylindrical containers, 895 mm wide, is then consolidated in four successive layers. After consolidation, the 350 inclusions are jacked into the clay sample at a square mesh of 23 mm (2.3 m at prototype scale). The ballast layer is simulated by Fontainebleau sand pluviated on top of the clay (Figure 4).

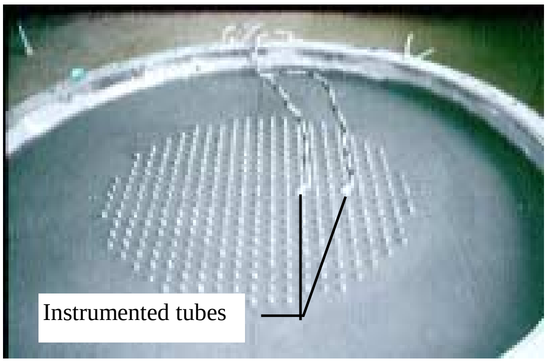

Figure 4. Inclusions jacked into the clay bed

The models are instrumented to measure :
- Pore pressures at different locations below the foundation
- Soil settlements
- Vertical and horizontal displacements of the footing
- Water table level (kept close to the clay layer surface)
- Applied loads (shear force and overturning moment)
- Bending moment in 2 or 3 inclusions (Figure 4).

A cone penetrometer actuator or a vane test device are located onto the container to determine the clay characteristics during the 100 g tests. For the clay used in the tests, a linear relationship has been obtained between CPT tip resistance q_c and undrained shear strength S_u both measured in flight:

$$S_u = q_c / 14.7$$

The loads applied to the foundation system have three independent components:
- vertical load V kept constant during the whole tests (V = 8.9 kN in Test 1 and 9.3 kN in Tests 2 and 3, in prototype conditions). This load is simulated by the dead weight of the foundation.
- horizontal shear force T applied at an elevation h=118 mm (11.8 m in prototype conditions) above the foundation level (top of the ballast layer). A hydraulic servo-actuator is used and the horizontal load T produces an overturning moment T.h.
- additional overturning moment M corresponding to a vertical load eccentricity. This overturning moment is obtained by displacing a carriage and a movable mass using an electric motor and an endless screw (Figure 3). The position of the carriage is monitored by a displacement transducer. An adjustable counterweight allows to balance all moments to zero when the movable mass is at its central position.

A typical loading path is shown in Figure 5 below.

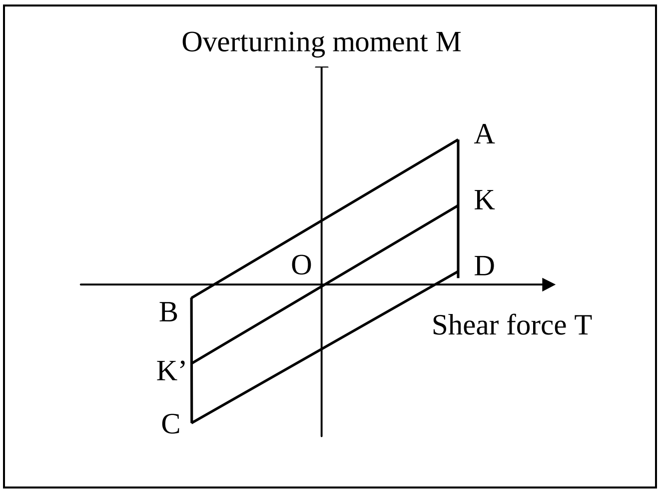

Figure 5. Typical load path

Path OK-OK' corresponds to cyclic horizontal shear force T when the vertical load is applied at the center of the foundation. Paths AB and DC are also cyclic shear force but the vertical load is eccentric (additional constant overturning moment). Paths AD and BC are cyclic overturning moment under a constant horizontal shear force T.

Table 1 presents the loading programs of the three tests. In order to be in undrained conditions in the clay beds, frequency for cyclic loading is chosen as 0.1 Hz in shear T loading and 0.02 Hz in combined T-M loading.

Table 1. Loading programs in Tests 1, 2 and 3 in prototype conditions

Test Sequence	Test 1	Test 2	Test 3
1	10 cycles T=+/-6.5 MN	10 cycles T=+/-5 MN	10 cycles T=+/-15 MN
2	10 cycles T=+/- 14 MN	10 cycles T=+/-15 MN	10 cycles T=+/-15 MN and M=+/-70 MN.m
3	10 cycles T=+/- 35 MN	10 cycles T=+/-15 MN and M =+/-70 MN.m	10 cycles T=+/-35 MN

4	Static loading T to failure	10 cycles T=+/-35 MN and M=+/-170 MN.m	5 cycles T=+/-35 MN and M=+/-170 MN.m
5		Static loading T up to failure	5 cycles T=+/-35 MN
6			Static loading T up to failure

5 TESTS RESULTS

Each clay model is consolidated at 100 g for two to five hours before starting the loading tests. The consolidation ratio at the end of this 100 g consolidation is close to U=100% in the upper reinforced layers. On the whole clay beds, U ranges from 74% to 95% depending on the clay sample.

Results of the CPT tests performed in flight in Test 2 at the end of the 100 g consolidation are shown in Figure 6 and compared to the shear strength profile observed on site:

$$S_u = 30 + 2.8\ z \quad (S_u \text{ in kPa, z in m})$$

It is obviously not possible to present all loading test results and only some data from Test 2 are shown as examples. First, Figure 7 gives the main recorded values vs. time in model units. The loading sequences 1 to 5 indicated in Table 1 are clearly seen in the shear force T vs. time curve.

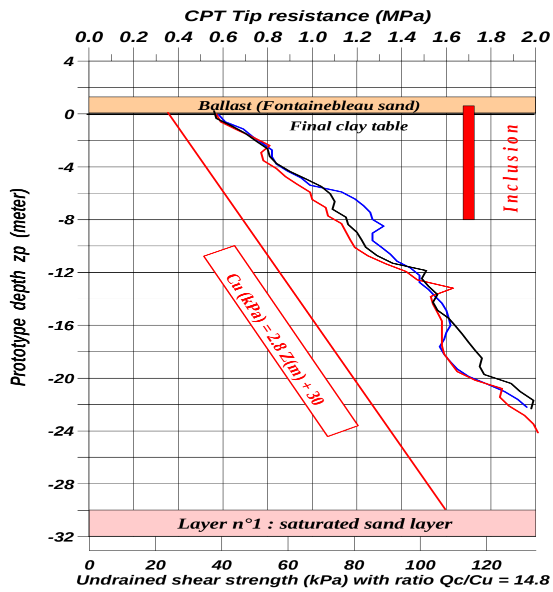

Figure 6. Shear strength profiles from in flight CPT tests performed into the clay sample (Test 2)

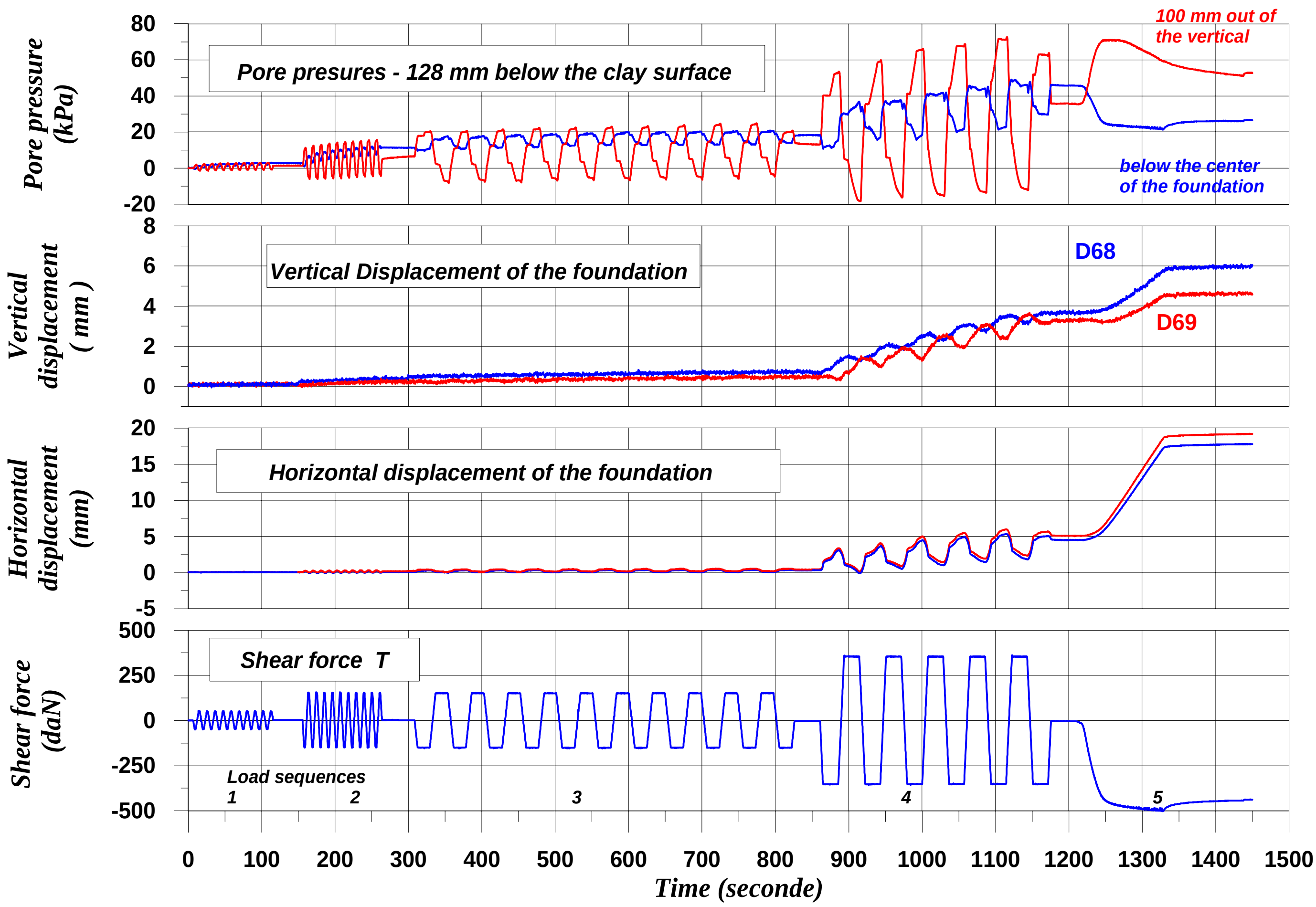

Figure 7. Test 2: horizontal load T, vertical and horizontal foundation displacements, pore pressure vs. time in model conditions.

An example of relationship observed between foundation displacement and cyclic shear force is shown in Figure 8 corresponding to sequence 2. In this case, large hysteresis is seen but displacements stabilize with cycles.

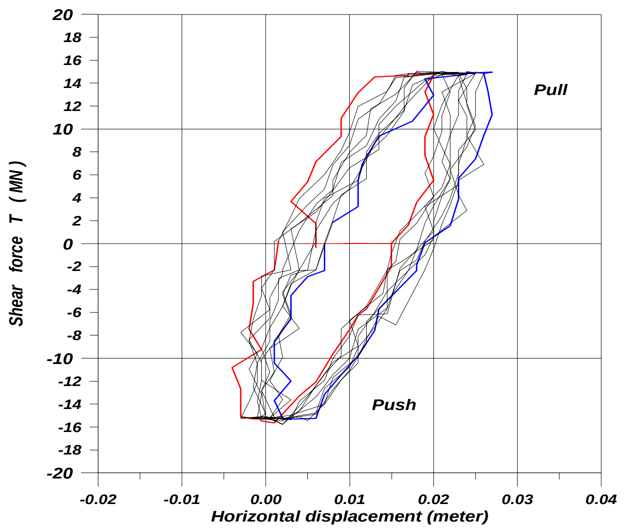

Figure 8. Test 2 : Horizontal displacement of the foundation vs. cyclic shear force T (sequence 2)

Tests have also shown that pore pressures may develop during loading. Figure 9 gives measurements done during sequence 4 by a PPT placed 12.8 m deep in the clay and 10 m out of the vertical of the center of the foundation in the direction of loading. The pore pressure variation due to the five cycles goes from - 20 kPa to +80 kPa. It is sensitive to both the additional overturning moment M and to the shear force T.

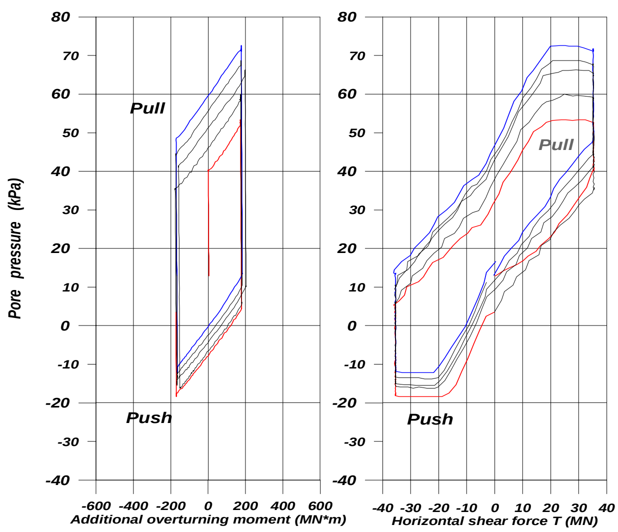

Figure 9. Test 2: Excess of pore pressure due to cyclic loading 12.8 m deep in the clay and 10 m out of the vertical of the foundation in the loading direction (sequence 4).

The inclusions participate significantly in the response of the foundation system even under relatively small loads. Figure 10 presents the bending moment profiles observed in inclusion P5 during static loading up to failure (sequence 5). This 8.5 m long inclusion is placed at a distance of 13.8 m from the center of the foundation in the loading direction (Figure 12). Maximum bending moment is located at mid-depth and increases with the applied horizontal shear force. When the load reaches T = 45 MN, bending moment in inclusion increases much more rapidly.

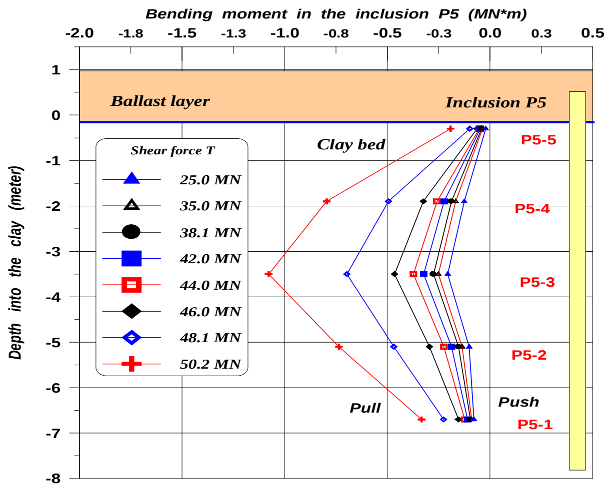

Figure 10. Test 2 : Bending moment vs. depth in inclusion P5 during loading sequence 5

This critical load about 45 MN is also observed in the load vs. foundation displacement plotted in Figure 11. This figure presents the response of the foundation system to the final static T loading up to failure (sequence 5 in table 1). At the beginning of sequence 5, the horizontal displacement of the foundation is 0.48 m due to the previous cyclic sequences 1 to 4.

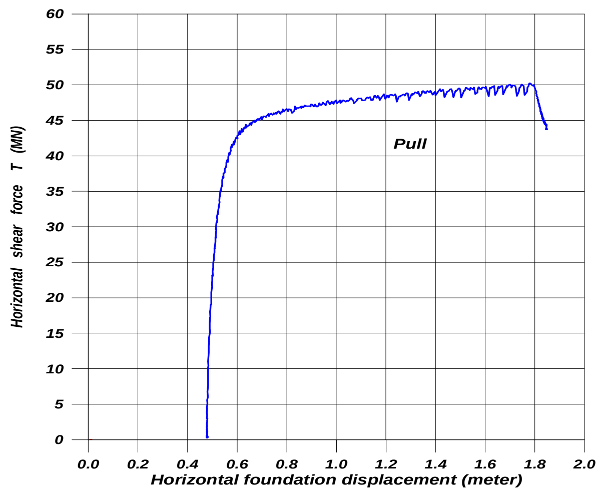

Figure 11: Test 2: Horizontal shear force vs. foundation displacement in loading sequence 5

The loading curve in Figure 11 indicates a very stiff response up to a load about 43 MN at which the relative horizontal displacement is only 0.12 m. Displacement increases more rapidly after this T=43 MN load that corresponds to failure. The displacement controlled loading process continues up to a horizontal displacement of 1.32 m (1.8 m from the beginning of the test). The carried shear force T is then close to 50 MN.

A view of a vertical cut done in the model after the centrifuge loading test is shown in Figure 12. The print of the circular footing is clearly seen and the figure also indicates that clay deformation and inclusions rotation are much larger at the front of the footing in the loading direction.

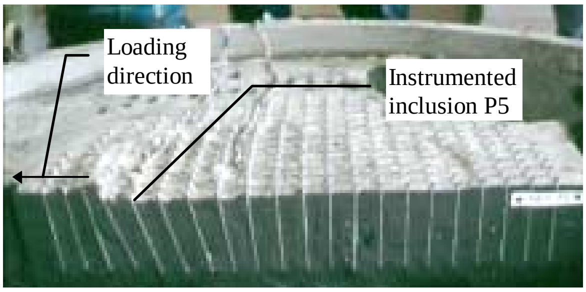

Figure 12. Test 2 : Vertical cut of the model after the loading test along the footing diameter in the loading direction.

All three loading tests of foundation resting on the reinforced clay have shown that neither the initial stiffness nor the ultimate resistance to horizontal loads are affected by the previous cyclic loading sequences even if some have been very severe.

6 COMPARISON WITH THEORETICAL ANALYSES

The theoretical tools developed to analyze the behavior of the reinforced soil are based on a limit analysis method (yield design theory; Salençon 1990) and on the finite element method. The yield design theory allows the determination of the ultimate loads that the foundation can withstand and therefore provides a means of estimating the ultimate bearing capacity under various monotonic load paths. The finite element analyses give additional information, the displacements and the rotations of the foundation, and provide a means of estimating its seismic behavior.

Due to the space limitations, the results of the centrifuge tests will be compared only to those of the yield design theory. Figure 13 presents the kinematic mechanism used in the yield design theory (Pecker, Salençon 1998). Under the combined effect of the vertical load, horizontal shear force and overturning moment, the foundation undergoes a rotation around point Ω, uplift along its left edge and the inclusions under the right edge are strained and displaced; the maximum bending moment occurs approximately at mid-height of the inclusions, at the intersection of the inclusions and of the kinematic mechanism. These results predicted by the yield design theory are in very good agreement with those observed during the centrifuge test: see figures 10 and 12 for comparison (taking into consideration that in figure 12 the load is acting to the left whereas in figure 13 it is directed to the right).

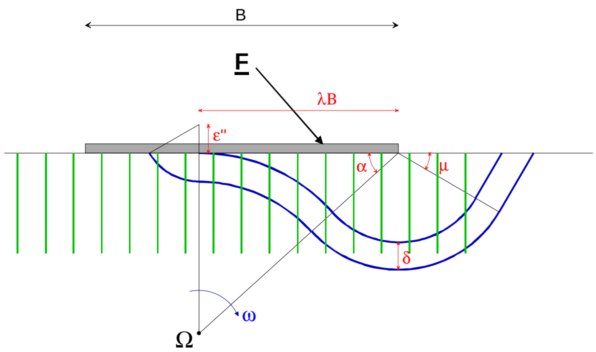

Figure 13. Kinematic mechanism

It is interesting to note that the finite element analyses predict the same failure mechanisms.

For the three tests carried out in the centrifuge facility in Nantes and for five other tests carried out in another centrifuge facility in Bordeaux, the results of which are not reported herein, figure 14 presents the comparison between the computed failure loads (yield design theory) and the measured ones. In Nantes, those failure loads were measured after cyclic loading, whereas in Bordeaux, they were measured without any prior cyclic loads. In Nantes, the testing arrangement is identical between the three tests and the load paths are varied; in Bordeaux, the load path is identical in the five tests but the other parameters are varied (number of inclusions, soil strength, vertical load). It appears from figure 14 that the trends are correctly predicted, that the predictions and measurements are in very good agreement for the Nantes tests and that the failure loads are underestimated for the Bordeaux tests. However, during the tests in Bordeaux, it was noticed that at failure, significant changes in the initial geometry of the system (formation of a soil bulging at the front of the foundation) occur and that the failure loads were measured at very large displacements. If the "failure" loads are taken at the start of the changes in geometry, the agreement between predictions and measurements is also very good.

Figure 14. Comparison of measured and computed

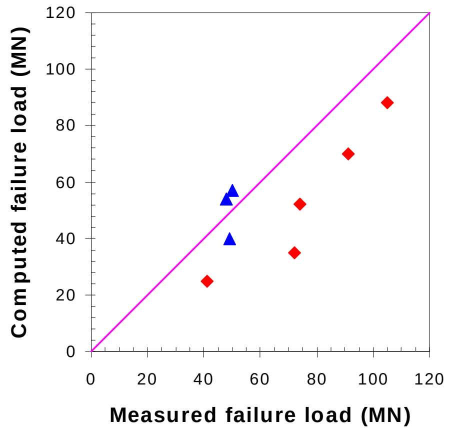

failure loads

Finally, the cyclic tests have shown that the system exhibits a significant energy dissipation capacity with the formation of fat hysteresis loops during cyclic loading. The equivalent damping ratio computed from the hysteresis loops of figure 8 is equal to 18%, whereas the theoretical predictions from the finite element analyses are of the order of 15% at the same load level.

In addition, even at very high cyclic load levels (75% to 80% of the failure load), the system exhibits very small degradation; the hysteresis loops stabilize after a few number of cycles (figure 8); the permanent excess pore pressure is only a small fraction (30%) of the initial hydrostatic pressure.

7 CONCLUSION

The centrifuge model tests have permitted the validation of this innovative foundation concept proposed for the foundations of the Rion Antirion bridge. In addition, they were used to calibrate the theoretical analyses and numerical tools developed for the design of the foundations which requires extensive parametric studies, which cannot obviously be carried out with the model tests.

REFERENCES

Combault J., Morand P. 1998. The exceptional structure of the Rion Antirion bridge in Greece. *Proceedings of the IABSE Conference* - Kobe (Japan).

Corté J.F., Garnier J. 1986. Une centrifugeuse pour la recherche en géotechnique. *Bull. Liais. Labo. P. et Ch.* 146: 5-28

Pecker A., Teyssandier J.P. 1998. Seismic design for the Rion Antirion Bridge", *Proc. Instn. Civ. Eng. Geotech. Engng.*, 131 pp. 4-11 - Paper 11311.

Pecker A 1998. Capacity design principles for shallow foundations in seismic areas. *Keynote lecture, Proceedings XIth Europ. Conf. on Earthquake Engineering*. Eds. Bisch, Labbé, Pecker - Balkema.

Pecker A., Salençon J. 1998. Innovative concepts in foundation engineering. *2nd Japan-UK Workshop on implications of recent earthquakes on seismic risk*, Tokyo Institute of Technology, April 6-9, 1998.

Salençon J. 1990. Introduction to the yield design theory. *European Journal of Mechanics A/Solids 9*, n° 5, pp. 477-500.